JOURNAL OF SOLID STATE CHEMISTRY 69, 126–134 (1987)

Sodium Ion-Conducting Solid Electrolytes in the System Na_3PO_4–Na_2SO_4

J.T.S. IRVINE AND A.R. WEST

Department of Chemistry, University of Aberdeen, Meston Walk, Aberdeen AB9 2UE, United Kingdom

Received August 15, 1986

In the system Na_3PO_4–Na_2SO_4, the high-temperature, cubic γ form of Na_3PO_4 forms an extensive range of solid solutions: $Na_{3-x}(P_{1-x}S_x)O_4$, $0 < x <$ (0.57 to 0.70, depending on temperature). For compositions in the range x = ca. 0.33 to 0.57, these γ solid solutions are thermodynamically stable at all temperatures. The conductivity of the γ solid solutions increases with increasing x and reaches a maximum at x = 0.5 to 0.6, with values of 2×10^{-5} ohm^{-1} cm^{-1} at 100°C, rising to 1.3×10^{-2} ohm^{-1} cm^{-1} by 300°C; this conductivity increase with x is attributed to an increase in the sodium ion vacancy concentration, associated with the solid solution mechanism Na + P $\rightleftharpoons$ S. The phase diagram for the system Na_3PO_4–Na_2SO_4 is given together with lattice parameters of the γ solid solutions. © 1987 Academic Press, Inc.

Introduction

Sodium orthophosphate, Na_3PO_4, is the parent end-member of several solid solution series which have potential as sodium ion-conducting solid electrolytes. The highest conductivity found so far in these systems is in zirconium-doped materials, with a conductivity at 300°C of 0.025 ohm^{-1} cm^{-1} for the composition $Na_{2.5}Zr_{0.125}PO_4$ (*1*). Pure Na_3PO_4 has only a modest conductivity, ca. 10^{-5} ohm^{-1} cm^{-1} at 300°C for the tetragonal α polymorph, increasing to ca. 10^{-4} ohm^{-1} cm^{-1} at 350°C for the cubic γ polymorph (*2*). The structure of the cubic form may be described as either derived from the Li_3Bi structure (*3*), which is essentially an ordered CsCl structure, or a cation excess antifluorite structure (*4*). An explanation of the enhanced conductivity in the Zr-doped materials is associated with the introduction of vacancies into the excess sodium sites (*1*).

Studies of the system Na_3PO_4–Na_2SO_4 (*5–7*) have shown the existence of an extensive range of cubic, γ-Na_3PO_4 solid solutions (*5–7*) but with conflicting results on the conductivity of these solid solutions. One study (*5*) found no enhancement of conductivity but another (*7*) found greatly enhanced conductivity at temperatures around ambient. Two of these studies (*6, 7*) reported the lattice parameters of the Na_3PO_4 solid solutions as a function of composition but gave very different results. In this paper, we report a systematic study of the solid solutions that form in this system, their stability in terms of the phase diagram, X-ray lattice parameter data, and conductivity data.

Experimental

Starting materials were Na_2CO_3, $NH_4H_2PO_4$, and Na_2SO_4 (all Analar grade). The sulfate and carbonate were dried at

0022-4596/87 $3.00

Copyright © 1987 by Academic Press, Inc.
All rights of reproduction in any form reserved.

200°C and stored in a desiccator. Mixtures were prepared in ca. 15-g amounts, ground together with acetone, dried, and fired in Pt crucibles in electric muffle furnaces. The firing temperatures were 200°C for ca. 3 hr, 650 to 800°C for ca. 3 hr, and 850°C for 2 days. These conditions were found to give equilibrium products, as shown by subsequent phase diagram studies. For the phase diagram work, some samples (ca. 25 mg wrapped in Pt foil) were quenched rapidly from high temperatures by dropping into Hg. Melting temperatures were estimated by noting the appearance of pelleted samples after heating at various temperatures for ca. 10 min.

Thermal analyses (DTA, TG) were carried out on a Stanton Redcroft 1500°C combined DTA/TG instrument, using alumina as reference with heating and cooling rates of 10°C/min. Phase analysis was carried out by X-ray diffraction using a Philips Hägg Guinier powder camera, CuK_{α_1} radiation. For accurate d-spacing measurements, KCl was added to the sample as an internal standard and the films were measured using a Cooksley microdensitometer.

For conductivity measurements, pellets were cold pressed and sintered at temperatures in the range 850 to 1000°C, depending on composition, for 2 days. Electrodes were fabricated from organogold paste which was fired onto the pellets at 200 to 600°C. The pellets with their gold electrodes were attached to Pt leads in a conductivity cell which was then placed inside a horizontal tube furnace. Measurements were made over the temperature range ambient to 500°C in an atmosphere of either laboratory air or nitrogen. Temperatures were controlled and measured to within 2°C. ac impedance measurements were made using a Solartron 1250 frequency response analyzer linked to a Solartron 1286 Electrochemical Interface and controlled from a BBC microcomputer. The frequency range was usually 1 Hz to 65 kHz and the voltage applied across the sample was 0.1 V. Data were presented in the various impedance, admittance, and electric modulus formalisms, as appropriate, in order to identify the equivalent circuit of the sample and obtain values for the component R and C parameters. At high temperatures, the resistance of the leads made a significant contribution to the total resistance of the cell and an appropriate correction was made to the data in order to eliminate the effects of lead resistance.

Results and Discussion

The Phase Diagram Na_3PO_4–Na_2SO_4

The phase diagram has been determined approximately using a combination of X-ray diffraction on quenched, heat-treated samples, melting observations on pelleted samples, and combined DTA/TG. The result is shown in Fig. 1; many of the boundary curves have not been determined with certainty and are shown dashed.

At high temperatures, an extensive range of cubic, γ-Na_3PO_4 solid solutions forms with formula $Na_{3-x}(P_{1-x}S_x)O_4$. The sulfate-rich limit is x = ca. 0.57 at low temperatures but the solid solutions probably extend to higher x at higher temperatures,

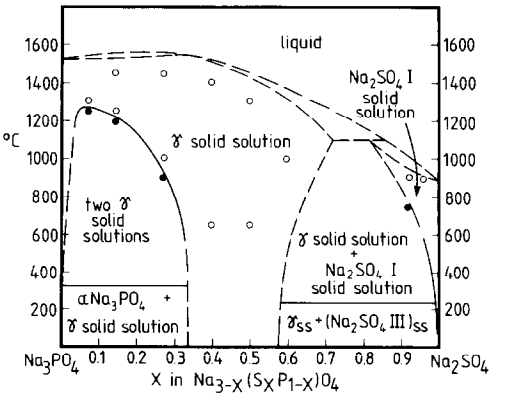

FIG. 1. Phase diagram for the system Na_3PO_4–Na_2SO_4; ○, one phase present in quenched samples; ●, two phases present in quenched samples.

with a limiting x of ca. 0.7 at 1050°C. Evidence for the existence of these latter solid solutions with $x > 0.57$ was indirect, from DTA and melting studies; quenched samples of these compositions, $x > 0.57$, showed a mixture of γ and Na_2SO_4, indicating that exsolution had occurred rapidly on cooling and could not be prevented.

At lower x values, ca. 0 to 0.3, and lower temperatures, less than ca. 1250°C, the γ solid solutions become unstable and enter a dome of immiscibility. For most of these compositions, the high-temperature, single-phase γ solid solutions that exist above the immiscibility dome could be quenched intact to ambient; hence, it was possible to determine the locus of the immiscibility dome by quenching samples from different temperatures and noting whether one or two phases were present in the X-ray powder patterns. The relevant results for three compositions are indicated in Fig. 1.

The immiscibility dome is rather asymmetric and has its upper consolute point at x = ca. 0.07 and 1275°C. The locus of the dome could not be determined for x smaller than 0.07 since it was not possible to quench the single-phase γ solid solutions intact for these γ solid solution compositions. The sulfate-rich limit of the dome is estimated as x = ca. 0.33.

Inside the immiscibility dome, two regions are identified in Fig. 1 above and below ca. 320°C. These regions are distinguished by the polymorphism of essentially stoichiometric Na_3PO_4. The $\gamma \rightarrow \alpha$ transformation was nonquenchable for compositions close to and including Na_3PO_4, and therefore, in the region of the dome greater than ca. 320°C, the low-sulfate γ component of the mixture of two γ solid solutions transformed to the α form during quenching. The $\alpha \rightleftharpoons \gamma$ transformation was followed by DTA and the peak temperature (320°C) that was found is similar to that reported for stoichiometric Na_3PO_4 (*8*). From the DTA and X-ray results, there was no evidence for any significant solid solution of Na_2SO_4 in the α form of Na_3PO_4.

The melting point of the γ solid solutions appeared to pass through a slight maximum at compositions around 33% Na_2SO_4. This composition also coincides approximately with the sulfate-rich limit of the immiscibility dome at low temperatures. These two pieces of evidence indicate the possible presence of an "ideal" composition of special stability with the likely formula $33.3Na_2SO_4$ and $66.7Na_3PO_4$, or $Na_{2.67}(P_{0.67}S_{0.33})O_4$.

The melting curves are shown as dashed lines and were drawn based on the results of melting experiments on cold-pressed pellets. For each composition, the onset of melting was noted (Table I) and taken to represent some temperature intermediate between the solidus and liquidus. The value obtained for pure Na_3PO_4, 1525 to 1535°C, agrees reasonably well with the literature value of 1512°C (*9*). No attempts were made to obtain melting temperatures by DTA since TG results showed that signifi-

TABLE I

RESULTS OF MELTING EXPERIMENTS ON PELLETED Na_3PO_4–Na_2SO_4 SAMPLES

Composition, % Na_2SO_4	Onset of melting
0	1525–1535
0.073	1525–1535
0.143	1535–1550
0.273	1550
0.40	1500
0.50	1400–1450
0.55	1350–1400
0.57	1350–1400
0.60	1300–1350
0.66	1250–1275
0.70	1200–1225
0.75	1150–1175
0.80	1100–1150
0.85	1050–1100
0.92	950–1000
1.00	875– 900

cant weight loss occurred at high temperatures. For instance, for compositions x = 0.14 or 0.55 the TG results showed weight loss commencing at ca. 1300°C, presumably associated with volatilization of the more volatile, lower melting, sulfate component.

At the sulfate-rich end of the diagram, there was evidence for a limited range of solid solutions in the high-temperature, hexagonal I form of Na_2SO_4. Precipitation of the γ phase from these solid solutions occurred rapidly on cooling, but could be prevented by quenching from high temperatures, as shown in Fig. 1 for two compositions. The melting temperatures of pellets increased with increasing Na_3PO_4 content, providing further evidence for the existence of a range of Na_2SO_4 solid solutions.

The phase diagram in the range x = ca. 0.6 to 0.9 is schematic. Complete solid solution between phosphate and sulfate at high temperatures is not possible since they have different crystal structures. However, the two-phase region (γ + sulfate I or III), which covers the composition range ca. 57 to 100% Na_2SO_4 at low temperatures, must narrow greatly at higher temperatures. Evidence for this narrowing, involving the dissolution of γ in sulfate and/or vice versa, was obtained by DTA (Fig. 2). A broad endotherm was seen on heating at temperatures in the range ca. 700 to 900°C. This effect was usually observed on cooling as an exotherm (not shown), but was broader than on heating and displaced to lower temperatures by ca. 80 to 90°C. This essentially reversible heat effect is attributed to the solution/exsolution processes. The endotherm was seen only for those compositions in the range x = ca. 0.60 to 0.98 and was largest for intermediate compositions, x = 0.85 and 0.92, in this range.

There was no evidence from the DTA and X-ray results for any solid solution in the low-temperature, III polymorph of Na_2SO_4. The DTA traces of sulfate-rich compositions (Fig. 2) showed an endothermic peak on heating at ca. 235°C that is attributable to the phase transition III → I and the peak temperature was the same for pure sulfate as in the sulfate component of two-phase mixtures. The sensitivity of DTA to this transition meant that the presence of small amounts of sulfate could be detected by DTA; in particular, it confirmed that the composition x = 0.6 contained some sulfate in samples that had been cooled slowly to ambient.

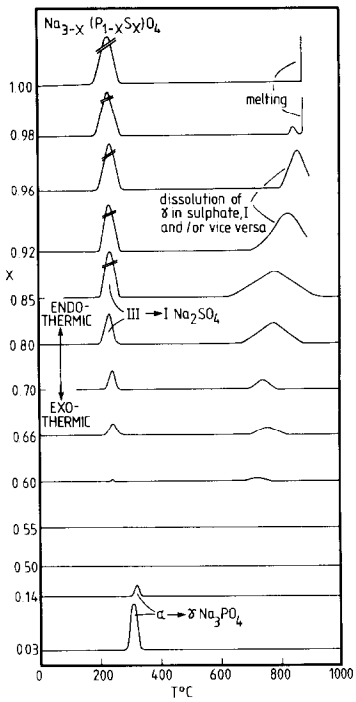

FIG. 2. Semischematic DTA traces obtained on the heating cycle.

DTA traces for some other compositions are shown in Fig. 2 and are interpreted, consistently with the phase diagram, as follows. For x = 0.03 and 0.14, some α-Na_3PO_4 was present, as evidenced by the peak at ca. 320°C. For compositions x = 0.50 and 0.55, there was no evidence of either the $\alpha \rightarrow \gamma$ phosphate peak at 320°C or the III → I sulfate peak at 325°C. These compositions therefore occur as a single-

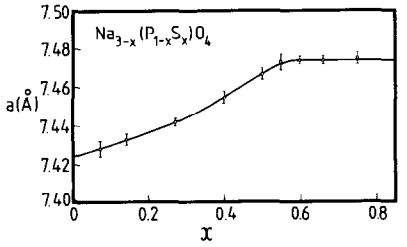

FIG. 3. Lattice parameter of the cubic γ solid solutions as a function of composition.

phase, γ solid solution at all temperatures below the melting point.

Lattice parameters of the γ solid solutions, determined from the *d*-spacings of the first six lines in the X-ray powder patterns, are shown in Fig. 3. For compositions in the range $x = 0.07$ to 0.27, samples were prepared by quenching from high temperatures to ensure that they were single-phase γ solid solutions. Data are not available for pure Na_3PO_4, $x = 0$, since it could not be quenched to room temperature as the cubic, γ polymorph. The data for the single-phase γ solid solutions, covering the range $x = 0.07$ to 0.55, fall on a smooth curve exhibiting downward curvature. Such downward curvature indicates that intermediate compositions have a smaller unit cell volume than is to be expected from a linear, Vegard's Law plot connecting the lattice parameters or unit cell volumes of the end-members. It indicates that these intermediate compositions may exhibit ordering effects in the solid solution structure and is further evidence in support of the existence of a "special" composition around $x = 0.33$.

For compositions $x > 0.60$, the lattice parameter is essentially constant, consistent with the observation that these materials are in the two-phase region of (γ + sulfate). These lattice parameter results indicate that the γ solid solution limit in our samples is 0.58 ± 0.02. The lattice parameters reported by Wiench and Jansen (*6*) are very similar to those found here with the differences that (a) the curvature in their a vs x plot is less pronounced and (b) they find evidence for solid solutions to higher x, 0.70. The explanation for the latter discrepancy is that perhaps Wiench and Jansen were successful in quenching to ambient the γ solid solutions in the range $x = 0.60$ to 0.70, which exist at high temperatures in the phase diagram (Fig. 1), whereas we were unsuccessful in quenching these sulfate-rich, γ solid solutions. Leaving aside these small differences, our two sets of data are in good agreement and very different from those of Majidi *et al.* (*7*), which show values of a in the range 7.39 to 7.435 Å, for $x = 0.10$ to 0.60, and passing through a minimum of 7.36 Å at $x = 0.23$.

Conductivity Results

The ionic conductivity of sintered, pelleted samples was measured satisfactorily over a range of temperatures using the ac impedance technique. For the majority of the samples, values for the bulk conductivity were readily determined and there was no evidence of significant grain boundary effects. The gold electrodes used were shown to be blocking to current flow and it was concluded that the current carriers in the pellets were sodium ions. These conclusions were deduced on the basis of the following.

The results were usually plotted in the complex impedance plane; typical results are shown in Figs. 4 and 5. For the majority of the samples, a single arc, approximating a semicircle, was observed at lower temperatures and higher frequencies, as in Figs. 4a and 4b, with a spike at higher temperatures and lower frequencies (Fig. 4c). The semicircle passed through the origin at high frequencies. Its associated capacitance, C_b, calculated from the relation $\omega RC = 1$ at the maximum of the semicircle, was ca. 1 pF cm^{-1}, indicating that the semicircle

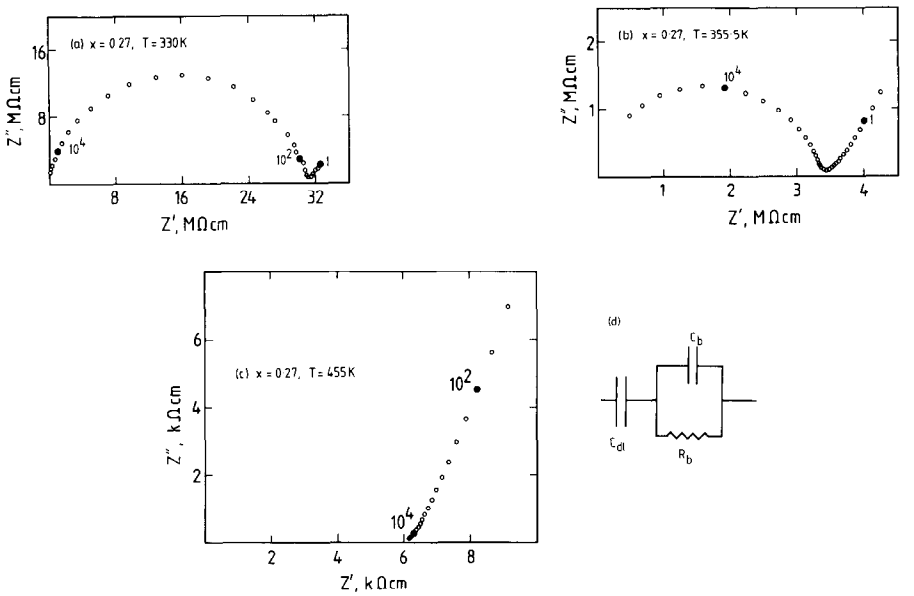

FIG. 4. Some typical ac impedance plots (a to c) and the equivalent circuit used to interpret the data (d). Selected frequencies, in Hz, are marked ●.

represented the bulk response of the pellet. The low-frequency intercept of the semicircle on the real, Z′ axis therefore represented the bulk resistance of the sample.

On the low-frequency side of the semicircle (Figs. 4b and 4c), the data took the form of an inclined spike. The value of the capacitance, C_{dl}, associated with the spike was estimated using the relation $Z'' = (1/\omega C)$. Values were typically ca. 2 μF, indicating that the spike represented polarization at the electrode–electrolyte interface.

There was no evidence, at intermediate frequencies, of any additional semicircles that could be attributed to, for instance, intergranular impedances. Hence, it was concluded that the electrical properties of the samples could be represented by the idealized equivalent circuit shown in Fig. 4d. This representation does not take into account deviations from "ideality" which manifest themselves as either distortions in the shapes of semicircles and/or deviations of spikes from the vertical. Such deviations were, in fact, apparent in the data but did not affect either the overall conclusions regarding the electrical makeup of the pellets or the extraction of resistance values from the intercepts of the semicircle/spike on the real, Z' axis.

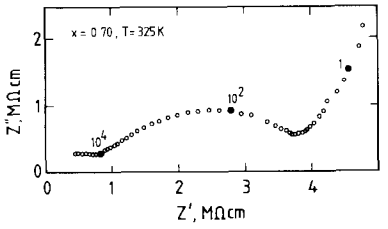

FIG. 5. Typical ac impedance plot for a sample showing both bulk and grain boundary effects.

It was concluded that the species responsible for the conductivity of the pellets are sodium ions. If, instead, either electrons or oxide ions were the principal current carriers, then the occurrence of a blocking, double-layer capacitance in the impedance response would not be expected.

Plots such as those shown in Fig. 4 were obtained for all compositions in the range $x = 0$ to 0.57. Samples with $x = 0.33$ to 0.57

would have contained a single γ solid solution phase at all temperatures and, hence, a single bulk semicircle is to be expected for these compositions. Samples with x = ca. 0.02 to 0.30 would have contained a mixture of γ solid solution of composition x = ca. 0.33 and essentially pure Na_3PO_4, and yet these samples also showed a single bulk semicircle, as in Fig. 4. For these compositions, it is presumed that the more highly conducting component, the γ solid solution x = ca. 0.33, dominated the conductivity of the pellets; this point is returned to later.

The ac impedance of sulfate-rich compositions generally showed a different kind of response (Fig. 5). These compositions were those ($x > 0.60$) that gave mixtures of γ solid solution of composition $x = 0.57$ and Na_2SO_4 in samples cooled to room temperature. There was evidence in the complex impedance plane for two semicircles, instead of one, with again a spike at lower frequencies. The resolution of the two semicircles varied somewhat between the different compositions; the example shown in Fig. 5 is for a relatively well-resolved case. The two semicircles were attributed to bulk (γ solid solution) and grain boundary (Na_2SO_4), for the following reasons.

For a given temperature, the semicircle at higher frequencies had an associated capacitance of ca. 1 pF cm^{-1} and was attributed to the bulk conduction process. The semicircle at lower frequencies had an associated capacitance of ca. 300 pF cm^{-1} in cases where it was well resolved from the bulk semicircle and was attributed to a grain boundary impedance. The grain boundary semicircle was usually somewhat larger than the bulk semicircle for a given sample, indicating that the grain boundary resistance was 2 to 4 times that of the bulk. The volume fraction occupied by the grain boundary material may be estimated from the ratio of the bulk and grain boundary capacitances, since capacitance is inversely proportional to thickness. This ratio, 1:300, indicates that the grain boundary material takes the form of a thin layer whose average thickness is ca. 0.3% that of the bulk crystals. This thickness ratio, coupled with the ratio of the two resistances, may be used to estimate the relative resistivities of the bulk and grain boundary material. From this, it is calculated that the grain boundary resistivity is some three orders of magnitude higher than that of the bulk. It is concluded that the grain boundary material is essentially Na_2SO_4, consistent with the Arrhenius plots (Fig. 7), which show that the conductivity of Na_2SO_4 is three to four orders of magnitude lower than that of the γ solid solutions.

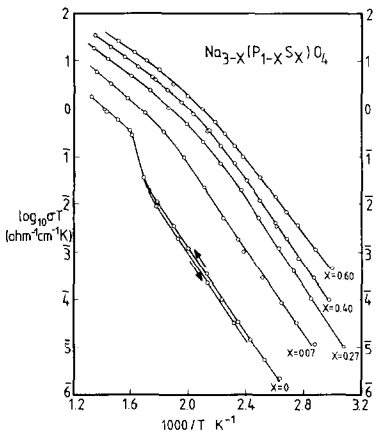

FIG. 6. Conductivity Arrhenius plots.

Bulk conductivities, extracted from plots such as those shown in Figs. 4 and 5, were used to construct Arrhenius plots of log σT against $1/T$ (Figs. 6 and 7). These are replotted as conductivity isotherms for four temperatures in Fig. 8, but as log σ instead of log σT. Most of the conductivity data (Figs. 6 and 7) fall into one of two linear regions and the activation energies and prefactors extracted from these are plotted against composition in Fig. 9.

The data for stoichiometric Na_3PO_4 (Fig. 6) show a discontinuity at ca. 300 to 320°C, which coincides with the transformation from the low-temperature, tetragonal α

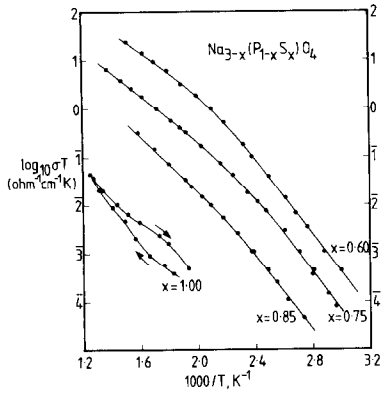

FIG. 7. Conductivity Arrhenius plots.

polymorph to the high-temperature, cubic γ polymorph. The conductivity data, with the discontinuity, were nearly reversible on the cooling cycle. These conductivities are considerably less than those reported by Hooper *et al.* (*5*). However, the latter were obtained on material prepared from commercial (technical) $Na_3PO_4 \cdot 12H_2O$ which probably contained significant amounts of NaOH as impurity (*10*).

On addition of Na_2SO_4 to Na_3PO_4, two effects are seen. First, the conductivities at all temperatures increase with x and pass through a maximum at x = ca. 0.6. The composition of this maximum also corresponds approximately to that of the sulfate-rich limit of the γ solid solution field. Second, the conductivity data for the solid solutions also show two linear regions. However, these linear regions are separated by a broad region of curvature, at temperatures in the range 100 to 300°C, depending on composition x, whereas for stoichiometric Na_3PO_4, the transition is more abrupt. For compositions x = 0.07 and 0.27, the pellets contained a mixture of two phases, Na_3PO_4 and γ solid solution of composition x = ca. 0.33, and it appears that the conductivity data given in Fig. 6 correspond to the more highly conducting, γ solid solution component of the pellets. A similar observation may be made for compositions x = 0.75 and 0.85. These contained a mixture of γ solid solution of composition x = ca. 0.57 and Na_2SO_4, but the conductivity data essentially correspond to those of the more highly conducting γ component of the pellets.

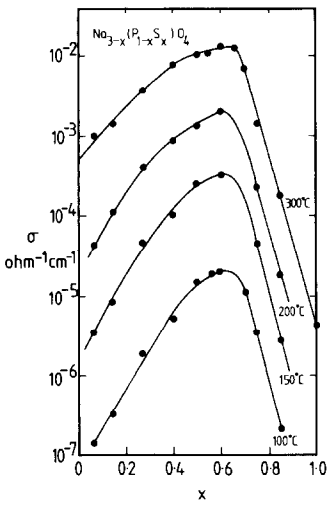

FIG. 8. Conductivity isotherms.

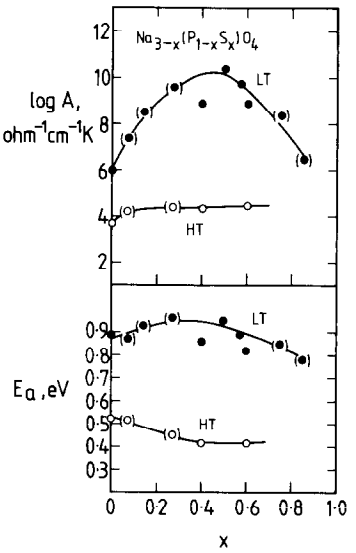

FIG. 9. Conductivity Arrhenius parameters as a function of composition. Data for samples that were not single phase are given in parentheses. LT = Low-temperature linear region; HT = high-temperature linear region.

The formation of the γ solid solutions by addition of Na_2SO_4 to Na_3PO_4 implies the solid solution mechanism

$$Na^+ + P^{5+} \rightleftharpoons S^{6+}$$

and hence the creation of sodium ion vacancies. These vacancies appear to be primarily responsible for the enhanced conductivity of the γ solid solutions with increasing x, particularly in the low-temperature region, where the prefactor A increases by about four orders of magnitude. It is assumed that the principal factor responsible for the variation in A is the carrier concentration; the activation energy in the low-temperature region is relatively constant with changing compositions and hence the entropy component of the prefactor is probably also relatively constant.

In the high-temperature region, the prefactor increases by about half an order of magnitude with increasing x at the same time that the activation energy shows a steady decrease; this increase in A is probably also associated with an increase in carrier concentration, but not such a large increase as in the low-temperature region.

The reason for the two linear regions, separated by a region of curvature, in the Arrhenius plots of the γ solid solutions appears to be associated with an order–disorder transition in the sodium ion site distribution. In stoichiometric Na_3PO_4, this is superposed on the displacive $\alpha \rightarrow \gamma$ transition at 320°C, but in the γ solid solutions, the structure is cubic at all temperatures. With increasing x, the region of curvature associated with this order–disorder transition moves to progressively lower temperatures, consistent with the expectation that the intrinsic disorder present in the low-temperature region also increases with x. It seems, therefore, that in the γ solid solutions, the transition is not from a state of complete order to one of complete disorder, but is instead from an essentially ordered state, with considerable disorder present, to an essentially disordered state, with considerable local order present.

Our conductivity values are broadly similar to those reported in the literature. Majidi *et al.* (*7*) measured conductivities over the temperature range 20 to 130°C; their values are close to ours although their activation energies are a little less (0.7 eV compared to 0.8 to 0.9 eV). Brice *et al.* (*2*) measured pure Na_3PO_4; the form and magnitude of their results are similar to ours but also with somewhat different activation energies (0.7 and 0.6 eV compared to 0.9 and 0.5 eV). Kumari and Secco (*11*), among others, have measured pure Na_2SO_4 and obtained similar magnitudes to ourselves, also showing a difference between heating and cooling cycles.

Acknowledgment

We thank the SERC for a research grant.

References

1. S. J. Milne and A. R. West, *Mater. Res. Bull.* **19,** 705 (1984).
2. J-F. Brice, B. Majidi, and H. Kessler, *Mater. Res. Bull.* **17,** 143 (1982).
3. D. M. Wiench and M. Jansen, *Z. Anorg. Allg. Chem.* **461,** 101 (1980).
4. J. M. Newsam, A. K. Cheetham, and B. C. Tofield, *Solid State Ionics* **1,** 377 (1980).
5. A. Hooper, P. McGeehin, K. T. Harrison, and B. C. Tofield, *J. Solid State Chem.* **24,** 265 (1978).
6. D. M. Wiench and M. Jansen, *Z. Anorg. Allg. Chem.* **486,** 57 (1982).
7. B. Majidi, J-F. Brice, and H. Kessler, *Mater. Res. Bull.* **19,** 1599 (1984).
8. M. Palazzi and E. Remy, *Bull. Soc. Chim. Fr.* **8,** 2795 (1971).
9. R. K. Osterheld and E. W. Bahr, *J. Inorg. Nucl. Chem.* **32,** 2540 (1970).
10. A. D. Mair, *New Zealand J. Sci.* **19,** 61 (1976).
11. M. S. Kumari and E. A. Secco, *Canad. J. Chem.* **61,** 2804 (1983).